AN ITAE OPTIMAL SLIDING MODE CONTROLLER FOR SYSTEMS
WITH CONTROL SIGNAL AND VELOCITY LIMITATIONS

Mateusz PIETRALA*, Piotr LEŚNIEWSKI*, Andrzej BARTOSZEWICZ*

*Institute of Automatic Control, Łódź University of Technology,
ul. Stefanowskiego 18., 90-537 Łódź, Poland

mateusz.pietrala@gmail.com, piotr.lesniewski@p.lodz.pl, andrzej.bartoszewicz@p.lodz.pl

Abstract: In this paper, a sliding mode controller, which can be applied for second-order systems, is designed. Robustness to external disturbances, finite regulation time and a good system's behaviour are required for a sliding mode controller. In order to achieve the first two of these three goals, a non-linear, time-varying switching curve is introduced. The representative point (state vector) belongs to this line from the very beginning of the control process, which results in elimination of the reaching phase. The stable sliding motion along the switching curve is provided. Natural limitations such as control signal and system's velocity constraints will be taken into account. In order to satisfy them, the sliding line parameters will be properly selected. However, a good dynamical behaviour of the system has to be provided. In order to achieve that, the integral time absolute error (ITAE) quality index will be introduced and minimised. The simulation example will verify theoretical considerations.

Key words: sliding mode control, optimal control, state constraints

1. INTRODUCTION

The sliding mode approach belongs to the class of variable structure control methodologies. The main idea is that the trajectory of the system state is constrained to a sub-space of the state space. This simplifies the dynamical behaviour of the system. Moreover, it allows us to obtain exceptional robustness with respect to external perturbations [6] and requires small computational effort. These advantages made sliding mode control profuse in the field of mechanical systems, electric drives and similar industrial applications. The fundamental concepts of this method were introduced in the previous century [20]; however, it remains a lively field of inquiry both from the practical [21] as well as theoretical [9] point of view.

Due to the discontinuous control signal, sliding mode control is especially useful in electric devices and power electronic control; as in these applications, the control signal (semiconductor switch state) is by its nature not continuous. The paper [7] presents a super-twisting sliding mode controller for speed control of permanent magnet synchronous machine (PMSM). The parameters of the controller are tuned on-line using a neural network to adapt to the varying, unknown disturbance values. The computer simulations as well as experimental tests confirm marked improvements over traditional sliding mode control as well as a PID (Proportional Integral Derivative) controller. The authors of [23] develop a sliding mode controller for a similar problem of linear PMSM control. In order to minimise chattering, it is enhanced by a neural network, which compensates the unknown impact of perturbations. To reduce chattering even further, the sign function in the controller is replaced by a time-varying saturation function, which determines the size of the boundary region to guarantee small error

and minimum chattering. The control methodology is verified on a laboratory stand and put alongside a sliding mode controller without the fuzzy logic extension. The results plainly demonstrate an improvement in control precision and oscillation reduction. In contemporary applications, it becomes increasingly common to control the plant through a network system, instead of a direct connection between each sensor/actuator and the controller. Such an approach can lower the costs and increase the modularity of the system. Unfortunately, it also presents some new difficulties, namely packet losses and transmission delays. In the work [8], an extensive review of modern sliding mode control algorithms that utilise networked control is presented.

In [10], a new sliding mode control approach was used in uninterruptible power supply (UPS) systems. The slope of the sliding line depends on the output voltage error via fuzzy logic. A simulation example demonstrated that the total harmonic distortion is lower than that in the strategy with the fixed sliding line. Furthermore, in [11], a laboratory experiment for the proposed strategy was performed. Terminal sliding mode control for two classes of non-linear systems was implemented in [16]. The first one comprises systems with the first- and second-order derivatives, and the second one included only first-order derivatives. The controller provided a finite reaching time and the stable sliding motion. Computer simulations included RLC (Resistor, Inductor, Capacitor) and RC (Resistor, Capacitor) plants with a non-linear resistor and capacitor. Terminal sliding mode control was also used for multi input multi output (MIMO) systems in [26]. The non-linear switching curve was selected in order to achieve a finite time convergence to the demand state.

The sliding mode approach is regularly applied not only in controllers but also in observers. One of its advantages is forcing the estimation error to zero in finite time [1, 17], in contrast to

asymptotic convergence in "traditional" observers. In the paper [5], the state of charge (SoC) estimation in a vanadium redox battery is considered. The authors begin by deriving a concentration model and tuning it using particle swarm optimisation. Next, it is transformed to the canonical control form, and a sliding mode observer is proposed. Since SoC in an actual battery is hard to measure directly, the battery voltage discrepancy between the observer and the real plant is used to assess the observation precision. What is more is the colour of the electrolytes in the full charge and discharge state verifies the observer performance. In the paper [4], the stator current and rotor flux linkage in a bearing-less induction machine is estimated via a sliding mode observer. Such motors have important advantages, resulting from replacing mechanical bearings by additional windings in the stator. With proper control of the current in the windings, radial forces can be developed, which make the rotor "levitate" inside of the stator. This allows the motor to attain significantly higher speeds and lowers friction force. A saturation function was used to reduce the chattering of the observer. The results of computer simulations show that the presented observer has faster convergence and lesser steady state error than the model reference adaptive system (MRAS) speed identification, which is typically used in its place. The sliding mode paradigm was also used in [12] both for observer and controller design for a gimbal control system for use in satellite orientation control. The performance is verified in simulations and in tests on a laboratory stand.

In the article [2], a sliding mode controller was implemented on a robotic manipulator. The reaching phase was eliminated by selecting the switching curve parameters in such a way that the initial state belongs to it. In the first example, the proposed strategy was applied to control the two-joint manipulator. The stable sliding motion was provided, and the convergence to the demand state is faster than that in previous methods. Moreover, the robustness to the external disturbances and modelling uncertainties was achieved. In the second example, the five-joint, bipedal manipulator was considered. A similar approach was implemented in [3], where the example with five-joint, bipedal manipulator was studied in greater detail. Moreover, the strategy was compared with a classical robot controller.

The control of unmanned aerial vehicles (UAVs) is recently very active and often utilises the sliding mode methodology. In the paper [24], quadrotor control is analysed. A reaching law comprising two hyperbolic functions is introduced. It enables on the one hand rapid convergence at a large distance from the switching hyperplane, while on the other hand it limits the risk of exciting oscillations in its vicinity. Then, a "system dynamics estimator" is derived in order to assess the wind impact. In general, using disturbance observers allows us to reduce chattering since it enables a reduction of the discontinuous portion of the control signal. The estimator design is grounded on the assumption of bounded variation of wind speed. Since in reality, the wind can come in gusts, it is not clear if this premise is realistic. Although the approach is tested on a real UAV, the tests are performed inside a laboratory, with constant wind speed simulated by a fan. Thus, it is unclear, how the proposed controller would perform in real conditions. A similar problem of UAV formation control was tackled in [19], where an adaptive non-singular terminal super-twisting sliding mode controller was proposed. One of the uses of UAV formation is inspection works, such as monitoring electric cables or solar panels. In the proposed approach, a sliding mode trajectory tracking controller for the formation leader is derived. Based on this trajectory, a formation controller produces trajecto-

ries for all of the following UAVs. Then, the same controller which was used for the leader is implemented in every follower. The robustness to wind perturbations is verified by computer simulations. The formation control problem was also analysed in [15] where a non-singular terminal sliding mode controller was designed. The major difference is that in [15] the authors assume that only local distance information is available, as not all followers are able to directly communicate with the leader. Furthermore, a collision avoidance mechanism was introduced, which is based on an artificial potential field. The concept was analysed in theory, as well as tested in computer simulations.

The topic of the paper [22] is control of a bridge crane. The authors propose a time-varying sliding mode controller. Similarly, as in this work, the sliding hyperplane initially passes through the starting state, which ensures robustness from the beginning of the control process. In the selected model, the movement of all the masses (the load, the hook and the trolley) are taken into account, while the main goal is to move the suspended load rapidly but not induce large oscillations in the system. The authors compare their approach with two methods with constant sliding hyperplanes in computer simulations. The advantages, namely improved robustness and smaller oscillations, are evident. The task of oscillation minimisation of moving masses was also considered in [25] where a benchmark problem of balancing a ball on a beam was analysed. The reaching phase was removed by using an integral sliding mode controller, while the sign function was smoothed out to reduce chattering. The laboratory tests confirm the impressive position control precision. In the paper [18], a second-order sliding mode controller for frequency control in a multi-area power system was derived. The unknown system states are first estimated using a linear observer. Then, a sliding mode controller utilises this information to reduce the frequency deviations.

While designing any practical controller, it is necessary to consider the constraints of the states and control action. One example is limiting the velocity in order to prevent mechanical damage. In our research, we came upon several methods which combine these bounds with sliding mode control. This motivated us to design such a sliding mode controller, which achieves good performance, despite limitations. This paper builds upon the previous work [13], by taking into account the minimisation of a different quality criterion. The method allows the designer to ensure a priori known bound on the system velocity and/or the control signal value.

2. SLIDING MODE CONTROLLER DESIGN

This section will present the sliding mode controller for the second-order system. During the design, we will focus on the following several main goals:
1. The robustness for the whole control process has to be obtained. It will be achieved by using a time-varying sliding curve, and as the result of a consequence, the reaching phase will be eliminated.
2. The state vector (representative point) has to reach the predetermined demand state in finite time.
3. External disturbances and natural restrictions such as control signal or velocity limitations have to be considered.
4. The integral time absolute error (ITAE) quality index has to be minimised in order to evaluate the performance of the controller.

Let us consider the following system:

$$\dot{\Theta}_1(\tau) = \Theta_2(\tau) \qquad (1)$$

$$\dot{\Theta}_2(\tau) = \Psi(\Theta_1(\tau), \Theta_2(\tau), \tau) + \Upsilon(\tau) + \xi v(\tau)$$

where $\Theta_1(\tau)$ describes the position of the system and $\Theta_2(\tau)$ is its velocity. Two functions Ψ (function of state vector and time τ) and Υ (external disturbances) vary in time. Nevertheless, due to the practical considerations, the absolute value of the sum of these functions has to be limited from above by a known, positive parameter denoted by Ω. This inequality can be written as follows:

$$|\Psi(\Theta_1(\tau), \Theta_2(\tau), \tau) + \Upsilon(\tau)| \le \Omega. \qquad (2)$$

The main advantage of using inequality (2) is that it allows to describe any bounded time-varying uncertainties. One does not have to assume any frequency distribution of the disturbances, which can be hard to obtain in practice. Positive scalar ξ affects the control signal v. The representative point starts moving from any position different from the desired one which is equal to 0, i.e $\Theta_1(0) \ne 0$ and $\Theta_2(0) = 0$. Moreover, it has to stop in the desired state. Therefore, the demand point is equal to $(0,0)$. The first goal that we mentioned in this section was the robustness for the whole control process and the elimination of the reaching phase. In order to achieve that goal, we introduce a time-varying, non-linear switching curve described by the following equation:

$$s(\tau) = \Theta_2(\tau) + \kappa(\tau)\, \text{sgn}(\Theta_1(\tau)) \sqrt{|\Theta_1(\tau)|}. \qquad (3)$$

The function κ corresponds to the variation rate of the sliding curve. The faster κ changes in time, the faster the sliding line evolves. Once κ ceases to change, the sliding line remains stationary. It is given as follows:

$$\kappa(\tau) = \begin{cases} \gamma\tau & for \quad \tau \le \tau_0 \\ \gamma\tau_0 & for \quad \tau > \tau_0 \end{cases}. \qquad (4)$$

Parameter γ is positive and denotes the movement speed of the switching curve. At the time τ_0, that curve stops and remains fixed. Sign function sgn is equal to 1 for positive arguments, is equal to 0 for 0 and is equal to -1 for negative arguments. Substituting $\tau = 0$ one can see that

$$s(0) = \Theta_2(0) + \kappa(0)\, \text{sgn}(\Theta_1(0)) \sqrt{|\Theta_1(0)|} = 0, \qquad (5)$$

which means that the representative point is on the sliding line at the initial state and the reaching phase is eliminated. It results in robustness to the external disturbances for the whole control process. In order to provide the stable sliding motion, we propose the following control signal:

$$v(\tau) = -\frac{1}{\xi}\, \text{sgn}(\Theta_1(\tau)) \sqrt{|\Theta_1(\tau)|} \frac{d}{d\tau}\kappa(\tau)$$

$$- \frac{\Theta_2(\tau)\kappa(\tau)}{2\xi\sqrt{|\Theta_1(\tau)|}} \frac{\Omega}{\xi}\, \text{sgn}(s(\tau)). \qquad (6)$$

Theorem 2.1 Control signal Eq. (6) provides the stable sliding motion for the whole control process. To prove the stability of the sliding motion, we have to guarantee that the following inequality

$$s(\tau)\dot{s}(\tau) \le 0 \qquad (7)$$

is fulfilled for any $\tau > 0$. The strict inequality is not necessary because the representative point is on the switching curve at the initial state. We determine the derivative of the sliding variable as follows:

$$\dot{s}(\tau) = \frac{d}{d\tau}\Theta_2(\tau) + \text{sgn}(\Theta_1(\tau)) \sqrt{|\Theta_1(\tau)|}\dot{\kappa}(\tau) + \frac{\Theta_2(\tau)\kappa(\tau)}{2\sqrt{|\Theta_1(\tau)|}} \quad (8)$$

Using Eq. (1), we obtain the following:

$$\dot{s}(\tau) = \Psi(\Theta_1(\tau), \Theta_2(\tau), \tau) + \Upsilon(\tau) - \Omega\, \text{sgn}(s(\tau)) \qquad (9)$$

From Eq. (2) and the sign function properties, we obtain that inequality (7) is true.

3. ADMISSIBLE SETS

In this section, three sets of the switching curve parameters that guarantee the control signal, system's velocity and both of these quantities limitation will be determined. These sets will be composed of two parameters: γ and τ_0. Moreover, we will cover two possible outcomes–when the sliding line stops during the control process and when the demand state is reached when it is still in motion. Let us start by deriving formulas for absolute values of both system's position and system's velocity. From Eq. (3) and the fact that the sliding variable is equal to zero, we have the following:

$$\Theta_2(\tau) = -\kappa(\tau)\, \text{sgn}(\Theta_1(\tau)) \sqrt{|\Theta_1(\tau)|}. \qquad (10)$$

Using Eqs (1) and (10), one can obtain the following:

$$\Theta_1(\tau) + \kappa(\tau)\, \text{sgn}(\Theta_1(\tau)) \sqrt{|\Theta_1(\tau)|} = 0 \qquad (11)$$

The above differential equation is fulfilled for

$$\sqrt{|\Theta_1(\tau)|} = \begin{cases} \delta_1 - \frac{\gamma\tau^2}{4} & for \quad \tau \in [0, \tau_0) \\ \delta_1 - \frac{\gamma\tau^2}{4} & for \quad \tau \in (\tau_0, \tau_f] \\ 0 & for \quad \tau \in (\tau_f, \infty) \end{cases} \quad (12)$$

where τ_f denotes the regulation time. System's position has to be a continuous function. Therefore, in order to fulfil that property, the absolute value of Θ_1 has to be of the following form:

$$|\Theta_1(\tau)| = \begin{cases} \left(\sqrt{|\Theta_1(0)|} - \frac{\gamma\tau^2}{4}\right)^2 & for \quad \tau \in [0, \tau_0) \\ \left(\sqrt{|\Theta_1(0)|} + \frac{\gamma\tau_0^2}{4} - \frac{\gamma\tau_0\tau}{4}\right) & for \quad \tau \in (\tau_0, \tau_f] \\ 0 & for \quad \tau \in (\tau_f, \infty) \end{cases} \quad (13)$$

and the regulation time is given as follows:

$$\tau_f = \frac{1}{2}\tau_0 + \frac{2\sqrt{|\Theta_1(0)|}}{\gamma\tau_0}. \qquad (14)$$

In order to derive the absolute value of the system's velocity, we use Eqs (10) and (13) and get:
$$|\Theta_2(\tau)| =$$

$$\begin{cases} \gamma\tau\sqrt{|\Theta_1(0)|} - \frac{\gamma^2\tau^3}{4} & for \quad \tau \in [0, \tau_0) \\ \gamma\tau_0\sqrt{|\Theta_1(0)|} + \frac{\gamma^2\tau_0^3}{4} - \frac{\gamma^2\tau_0^2\tau}{4} & for \quad \tau \in (\tau_0, \tau_f] \\ 0 & for \quad \tau \in (\tau_f, \infty) \end{cases} \quad (15)$$

In the second possible scenario, when the switching curve moves for the whole control process, we take into account only two time intervals. In this case, the absolute values of system's position and system's velocity can be written as follows:

DOI 10.2478/ama-2023-0026

acta mechanica et automatica, vol.17 no.2 (2023)
Special Issue "Modern Trends in Automation and Robotics in tribute to Professor Tadeusz Kaczorek"

$$|\Theta_1(\tau)| = \begin{cases} \left(\sqrt{|\Theta_1(0)|} - \frac{\gamma\tau^2}{4}\right)^2 & for \quad \tau \in [0, \tau_f) \\ 0 & for \quad \tau \in (\tau_f, \infty) \end{cases} \quad (16)$$

$$|\Theta_2(\tau)| = \begin{cases} \gamma\tau\sqrt{|\Theta_1(0)|} - \frac{\gamma^2\tau^3}{4} & for \quad \tau \in [0, \tau_f) \\ 0 & for \quad \tau \in (\tau_f, \infty) \end{cases}. \quad (17)$$

Regulation time is derived as follows:

$$\tau_f = \frac{2\sqrt[4]{|\Theta_1(0)|}}{\sqrt{\gamma}} \quad . \quad (18)$$

3.1. Control signal admissible set

In order to derive the admissible set in which the absolute value of the control signal is bounded from above the following inequality,

$$|v(\tau)| \le v_{max} \quad (19)$$

has to be fulfilled for any $\tau \ge 0$. Parameter v_{max} is the maximum admissible value of the control signal. After substituting Eqs (6)–(19), we obtain:

$$\left| sgn(\Theta_1(\tau)) \sqrt{|\Theta_1(\tau)|}\dot{\kappa}(\tau) + \frac{\Theta_2(\tau)\kappa(\tau)}{2\sqrt{\Theta_1(\tau)}} + \Omega\, sgn(s(\tau)) \right| \le |\xi|v_{max}. \quad (20)$$

Using properties of the absolute value, we can simplify the above inequality to the following form:

$$\left| \sqrt{|\Theta_1(\tau)|}\dot{\kappa}(\tau) - \frac{\kappa^2(\tau)}{2} \right| \le |\xi|v_{max} - \Omega. \quad (21)$$

Let us consider two possible movements of the representative point. In the first one, it moves along the fixed sliding line. In the second one, the representative point will be sliding on a moving switching curve.

1. The sliding line remains fixed.

Using the form of function κ given by Eq. (4), one can see that when the switching curve stops moving, it can be rewritten as follows $\kappa(t) = \gamma\tau_0$. Hence, $\dot{\kappa}(t) = 0$ and (21) can be rewritten as follows:

$$\frac{\gamma^2\tau_0^2}{2} \le |\xi|v_{max} - \Omega. \quad (22)$$

Transforming the above equation one can get

$$\tau_0 \le \frac{\sqrt{2(|\xi|v_{max} - \Omega)}}{\gamma}. \quad (23)$$

In order to derive the admissible set, we have to analyse the second scenario, when the sliding switching curve is in motion.

2. The sliding line moves.

Now the function κ takes the following form $\kappa(\tau) = \gamma\tau$, and its derivative can be expressed as follows $\dot{\kappa}(\tau) = \gamma$. Therefore, we can rewrite our boundary in the form:

$$\left| \gamma\sqrt{|\Theta_1(\tau)|} - \frac{\gamma^2\tau^2}{2} \right| \le |\xi|v_{max} - \Omega. \quad (24)$$

Inequality (22) from the previous scenario shows that $\left|\frac{\gamma^2\tau^2}{2}\right| \le |\xi|v_{max} - \Omega$ has to be true for $\tau \le \tau_0$. Parameters γ and τ are both positive; therefore, we will demand that inequality

$$\left| \gamma\sqrt{|\Theta_1(\tau)|} \right| \le |\xi|v_{max} - \Omega \quad (25)$$

is always true. The above equation can be transformed into the boundary of the parameter γ:

$$\gamma \le \frac{|\xi|v_{max} - \Omega}{\sqrt{|\Theta_1(0)|}}. \quad (26)$$

When the sliding line changes its position for the whole regulation process, we check the edge of the admissible set and obtain that

$$\gamma \le \frac{|\xi|v_{max} - \Omega}{2\sqrt{|\Theta_1(0)|}}. \quad (27)$$

One can see that the second inequality is more strict; therefore, we have to demand its fulfilment.

3.2. System's velocity admissible set

This subsection comprises the condition that has to be fulfilled to constrain the velocity of the system. We have to demand that for any $\tau \ge 0$ the following condition

$$|\Theta_2(\tau)| \le \Theta_{2max} \quad (28)$$

is satisfied. Let us start by considering the scenario when the switching curve moves. Hence, we will use the Eq. (17). We have to find the solution of the equation $\dot{\Theta}_2(\tau) = 0$. One can get

$$\gamma\sqrt{|\Theta_1(0)|} - \frac{3}{4}\gamma^2\tau^2 = 0. \quad (29)$$

From the above equation, we get that the maximum absolute value of the system's position is given as follows:

$$\max_{\tau>0}|\Theta_2(\tau)| = \frac{4\sqrt{3\gamma\sqrt[4]{|\Theta_1(0)|^3}}}{9}. \quad (30)$$

and is obtained at the time

$$\tau_{max} = \frac{2\sqrt{3\sqrt[4]{|\Theta_1(0)|}}}{3\sqrt{\gamma}}. \quad (31)$$

Therefore, the limitation on parameter γ can be written as follows:

$$\gamma \le \frac{27\Theta_{2max}^2}{16\sqrt{|\Theta_1(0)|^3}}. \quad (32)$$

In the second scenario, we do not have to consider the case when the sliding line is fixed. In this case, the maximum absolute value of the systems velocity is reached at the time τ_0 due to the shape of the switching curve. So, in this scenario, the constraint on the parameter γ is given as in Eq. (32).

3.3. Control signal and system's velocity admissible set

Taking into account both previous subsections one can write that the constraint on parameter γ in the case when the sliding line becomes fixed during the control process is given as follows:

$$\gamma \le \min\left\{\frac{|\xi|v_{max} - \Omega}{\sqrt{|\Theta_1(0)|}}; \frac{27\Theta_{2max}^2}{16\sqrt{|\Theta_1(0)|^3}}\right\}. \quad (33)$$

In the second scenario, when the switching curve moves, we have the following:

$$\gamma \le \min\left\{\frac{|\xi|v_{max} - \Omega}{2\sqrt{|\Theta_1(0)|}}; \frac{27\Theta_{2max}^2}{16\sqrt{|\Theta_1(0)|^3}}\right\}. \quad (34)$$

4. MINIMISATION OF ITAE QUALITY INDEX

This section comprises the evaluation of dynamical performance of the system by deriving and minimising the ITAE quality index in the presence of earlier mentioned constraints. This quality index takes the form:

$$I = \int_0^\infty |\Theta_1(\tau)|\tau d\tau. \tag{35}$$

From the fact that we have proven that our controller provides that the representative point reaches the desired state in the finite time, the above equation is given as follows:

$$E = \int_0^{\tau_0} |\Theta_1(\tau)|\tau d\tau. \tag{36}$$

In the first scenario, when the sliding line is fixed from some time of the control process, we use Eq. (13) and rewrite ITAE as follows:

$$E = \int_0^{\tau_0}\left(\sqrt{|\Theta_1(0)|} - \frac{\gamma\tau^2}{4}\right)^2 \tau\, d\tau + \int_{\tau_0}^{\tau_f}\left(\sqrt{|\Theta_1(0)|} + \frac{\gamma\tau_0^2}{4} - \frac{\gamma\tau_0\tau}{2}\right)^2 \tau\, d\tau. \tag{37}$$

After some calculations, we can express the above equation in the form:

$$E = \frac{1}{8}|\Theta_1(0)|\tau_0^2 - \frac{1}{48}\gamma\tau_0^4\sqrt{|\Theta_1(0)|} + \frac{1}{768}\gamma^2\tau_0^6 + \frac{\sqrt{|\Theta_1(0)|^3}}{3\gamma} + \frac{|\Theta_1(0)|^2}{3\gamma^2\tau_0^2}. \tag{38}$$

Our goal is to minimise this quality index. Therefore, we will equate the partial derivatives of ITAE with respect to γ and τ_0 to zero as follows:

$$\frac{\partial E}{\partial \gamma} = -\frac{1}{48}\tau_0^4\sqrt{|\Theta_1(0)|} + \frac{1}{384}\gamma\tau_0^6 - \frac{\sqrt{|\Theta_1(0)|^3}}{3\gamma^2} - \frac{2|\Theta_1(0)|^2}{3\gamma^3\tau_0^2}, \tag{39}$$

$$\frac{\partial E}{\partial \tau_0} = \frac{1}{4}|\Theta_1(0)|\tau_0 - \frac{1}{12}\gamma\tau_0^3\sqrt{|\Theta_1(0)|} + \frac{1}{128}\gamma^2\tau_0^5 - \frac{2|\Theta_1(0)|^2}{3\gamma^2\tau_0^3}. \tag{40}$$

Equating Eq. (40) to zero one can get the real form of γ as a function of τ:

$$\gamma = -\frac{4\sqrt{|\Theta_1(0)|}}{3\tau_0^2} \ \lor\ \gamma = \frac{4\sqrt{|\Theta_1(0)|}}{\tau_0^2}. \tag{41}$$

From the fact that γ and τ have to be positive, one can get that only the second value of γ in Eq. (41) belongs to the domain. Substituting this value to Eq. (39) and equating it to zero, we have:

$$-\frac{1}{24}\tau_0^4\sqrt{|\Theta_1(0)|} = 0. \tag{42}$$

Again, τ_0 is positive; therefore, the quality index has no stationary points, and as a consequence, the minimum is obtained on a boundary of the admissible set. In the second scenario, when the sliding line moves for the whole regulation process, the ITAE takes the form:

$$E = \int_0^{\tau_f}\left(\sqrt{|\Theta_1(0)|} - \frac{\gamma\tau^2}{4}\right)^2 \tau\, d\tau = |\Theta_1(0)|\frac{\tau_f^2}{2} - \frac{\gamma\tau_f^4}{8}\sqrt{|\Theta_1(0)|} + \frac{\gamma^2\tau_f^6}{96}. \tag{43}$$

Substituting the regulation time Eq. (18) one gets that the above equation can be rewritten as follows:

$$E = \frac{2\sqrt{|\Theta_1(0)|^3}}{3\gamma}. \tag{44}$$

Hence,

$$\frac{\partial E}{\partial \gamma} = -\frac{2\sqrt{|\Theta_1(0)|^3}}{3\gamma^2} \tag{45}$$

and we conclude that again ITAE has no stationary points; therefore, in both cases, the quality index is minimised on the boundary of the admissible set.

Minimisation of ITAE with control signal constraint In this subsection, the minimum value of ITAE with control signal limitation will be derived. We have already shown that ITAE is minimised on the boundary of the admissible set, i.e. on the lines $\gamma = \frac{|\xi|v_{\max}-\Omega}{\sqrt{|\Theta_1(0)|}}$ or $\tau_0 = \frac{\sqrt{2(|\xi|v_{\max}-\Omega)}}{\gamma}$. Substituting γ to the second equation in Eq. (41), we get:

$$\tau_0 = 2\sqrt{\frac{|\Theta_1(0)|}{|\xi|v_{max}-\Omega}}. \tag{46}$$

From the fact that the maximum value of τ_0 on this line is

$$\tau_0 = \sqrt{\frac{2|\Theta_1(0)|}{|\xi|v_{max}-\Omega}} \tag{47}$$

we obtain that the only stationary point does not belong to the admissible set. Therefore, the minimum value of ITAE will be obtained for the maximum possible value of τ_0 given by Eq. (47). Now let us focus on deriving the optimal parameters of the switching curve on the line $\tau_0 = \frac{\sqrt{2(|\xi|v_{\max}-\Omega)}}{\gamma}$. Substituting this value to Eq. (38), one gets the following:

$$E = \frac{|\Theta_1(0)|(|\xi|v_{max}-\Omega)}{4\gamma^2} - \frac{\sqrt{|\Theta_1(0)|}(|\xi|v_{max}-\Omega)^2}{12\alpha^3} + \frac{(|\xi|v_{max}-\Omega)^3}{96\gamma^4} + \frac{\sqrt{|\Theta_1(0)|^3}}{3\gamma} + \frac{|\Theta_1(0)|^2}{6(|\xi|v_{max}-\Omega)}. \tag{48}$$

Calculating the derivative of the right-hand side of the above equation and equating it to zero, we obtain the only stationary point:

$$\gamma = -\frac{\left(1+\sqrt[3]{2}+\sqrt[3]{4}\right)(|\xi|v_{max}-\Omega)}{2\sqrt{|\Theta_1(0)|}}. \tag{49}$$

From the fact that both $(|\xi|v_{\max}-\Omega)$ and $|\Theta_1(0)|$ are positive, we get that Eq. (49) is negative. Therefore, again, minimum of ITAE is obtained on the boundary of admissible set and is equal to the following:

$$E = \frac{65|\Theta_1(0)|^2}{96(|\xi|v_{max}-\Omega)}. \tag{50}$$

Optimal switching curve parameters are given as follows:

$$\begin{cases} \gamma = \frac{|\xi|v_{max}-\Omega}{\sqrt{|\Theta_1(0)|}} \\ \tau_0 = \sqrt{\frac{2|\Theta_1(0)|}{|\xi|v_{max}-\Omega}}. \end{cases} \tag{51}$$

In the second case, when the sliding line moves for the whole control process, ITAE is also minimised for the maximum value of $\gamma = \frac{|\xi|v_{\max}-\Omega}{2\sqrt{|\Theta_1(0)|}}$ and is expressed as follows:

$$E = \frac{4|\Theta_1(0)|^2}{3(|\xi|v_{max}-\Omega)}. \tag{52}$$

One can observe that E determined by Eq. (50) is smaller than the value of the same parameter given by Eq. (52). Hence, we can conclude that the optimal strategy is achieved when the sliding line moves, and after that, it becomes and remains fixed to the end of the control process.

4.1. Minimisation of ITAE using system's velocity constraint

Again, we will start by considering the strategy, when the switching curve stops during the control process. We have already shown that the minimum of ITAE is obtained on the boundary of the admissible set. Hence, it is equal to the following equation:

$$E = \frac{928|\Theta_1(0)|^3}{2187\Theta_{2max}^2}. \tag{53}$$

When the sliding line moves for the whole control process, then the minimum value of ITAE is written as follows:

$$E = \frac{32|\Theta_1(0)|^3}{81\Theta_{2max}^2}. \tag{54}$$

One can easily conclude that the value of Eq. (54) is smaller than that of Eq. (53). Hence, ITAE is minimised when the sliding line moves for the whole control process.

4.2. Minimisation of ITAE by using both control signal and system's velocity constraints

In this section, when the switching curve stops during the control process, we have to consider three possible cases:

1. $\gamma = \frac{|\xi|v_{max}-\Omega}{\sqrt{|\Theta_1(0)|}}$ and $\tau_0 = \sqrt{\frac{2|\Theta_1(0)|}{|\xi|v_{max}-\Omega}}$. In this case, the minimized ITAE is written as follows:

$$E = \frac{65|\Theta_1(0)|^2}{96(|\xi|v_{max}-\Omega)}. \tag{55}$$

2. $\gamma = \frac{27\Theta_{2max}^2}{16\sqrt{|\Theta_1(0)|^3}}$ and $\tau_0 = \frac{8\sqrt{3}|\Theta_1(0)|}{9\Theta_{2max}}$. Now ITAE is given by

$$E = \frac{32|\Theta_1(0)|^3}{81\Theta_{2max}^2}. \tag{56}$$

3. $\gamma = \frac{27\Theta_{2max}^2}{16\sqrt{|\Theta_1(0)|^3}}$ and $\tau_0 = \frac{16\sqrt{2(|\xi|v_{max}-\Omega)|\Theta_1(0)|^3}}{27\Theta_{2max}^2}$ In this case, the minimum value of ITAE can be expressed as follows:

$$E = \frac{64(|\xi|v_{max}-\Omega)|\Theta_1(0)|^4}{729\Theta_{2max}^4} - \frac{1024(|\xi|v_{max}-\Omega)^2|\Theta_1(0)|^5}{59049\Theta_{2max}^6} + \frac{2048(|\xi|v_{max}-\Omega)^3|\Theta_1(0)|^6}{1594323\Theta_{2max}^8} + \frac{16|\Theta_1(0)|^3}{81\Theta_{2max}^2} + \frac{|\Theta_1(0)|^2}{6(|\xi|v_{max}-\Omega)}. \tag{57}$$

Considering the second strategy, when the sliding line moves for the whole control process, we get the minimum value of ITAE as follows:

$$E = \max\left[\frac{4|\Theta_1(0)|^2}{3(|\xi|v_{max}-\Omega)}; \frac{32|\Theta_1(0)|^3}{81\Theta_{2max}^2}\right]. \tag{58}$$

One can observe that both Eqs (55) and (56) are always smaller than Eq. (58). Without knowing the values of initial parameters, we will not be able to state which of the three values such as Eqs (55), (56) or (57) will be the ITAE minimum. However, this value can be easily calculated when these parameters are given. The optimal strategy is the one: when the sliding line stops during the control process.

5. SIMULATION EXAMPLE

In this section, we will verify theoretical considerations by introducing the simulation. We present the following system:

$$\begin{cases} \dot{\Theta}_1(\tau) = \Theta_2(\tau) \\ \dot{\Theta}_2(\tau) = \frac{1}{\Pi}\sqrt{|\Theta_1(\tau)|}\arctan(\Theta_2(\tau)) + \Upsilon(\tau) + \xi v(\tau) \end{cases} \tag{59}$$

The representative point starts at (−4, 0). From the shape of the switching curve and stable sliding motion, one can conclude that the maximum value of Ψ is 1 due to the fact that $\frac{1}{\Pi}\arctan(\Theta_2(\tau))$ takes a value from [−1;1]. Absolute value of external disturbances is limited by 3. These disturbances switch 20 times per second between the minimum and maximum admissible value in order to provide the most difficult feedback from the controller. Therefore, Ω takes a value 4. We select parameter $\xi = 1$. We set limits of control signal and systems velocity as follows $v_{max} = 15$ and $\Theta_{2max} = 4$. Now, let us consider the first case in our paper: when the control signal is constrained. The minimum value of ITAE is

$$E = 0.9848 \tag{60}$$

and parameters related to the switching curve are given as follows:

$$\begin{cases} \gamma = 5.5 \\ \tau_0 = 0.8528s \end{cases} \tag{61}$$

Representative point reaches the demand state after $\tau_f = 1.2792s$. From the control signal chart shown in Fig. 1, one can observe that it takes its maximum admissible value at the start of a control process. After that, it switches with an amplitude equal to the value of parameter $\Omega = 4$. When the sliding line is in motion, the mean value of the input decreases monotonically. After time τ_0, it stops, and the control signal switches between its minimum admissible value and $-|v_{max} - 2\Omega|$ in order to maintain the stable sliding motion. When it reaches the demand state, it takes values 4 or −4 to remain in it. System position shown in Fig. 2 increases monotonically, and after time τ_f, its value is always equal to 0. System's velocity (Fig. 3) starts rising due to the fact that the object must accelerate in order to reach the demand state. After some time, it peaks and starts decreasing. At the time τ_0, we can see a non-differentiable point in our figure. It is the moment when the sliding line stops moving. Again, the demand state is reached in finite time τ_f. In the next scenario, when the absolute value of system's velocity is bounded from above, we get the optimal results when the switching curve moves for the whole control process. Minimum value of ITAE is

$$E = 1.5802 \tag{62}$$

and optimal parameter related to the speed of the switching curve is given as follows:

$$\gamma = 3.3750 \tag{63}$$

In this case, due to the fact that the sliding line moves for the whole control process, the control signal decreases monotonically. From Fig. 4, one can observe that in this scenario, it exceeds the value −15 because now we do not require the control signal limitation. After time $\tau_f = 1.5396\ s$, again it switches with amplitude Ω in order to maintain the representative point in a demand state.
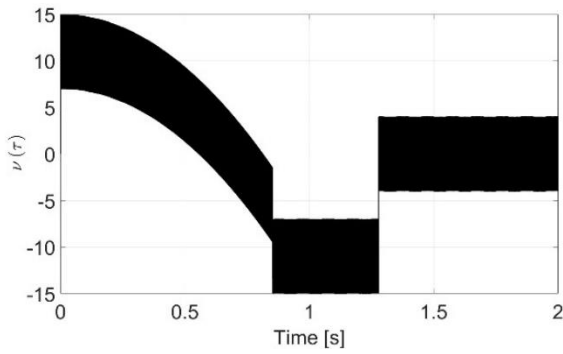
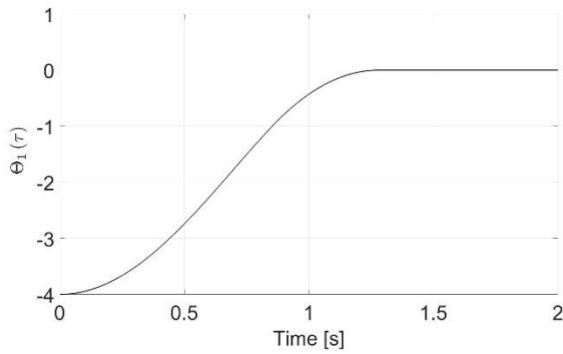**Fig. 1.** Control signal
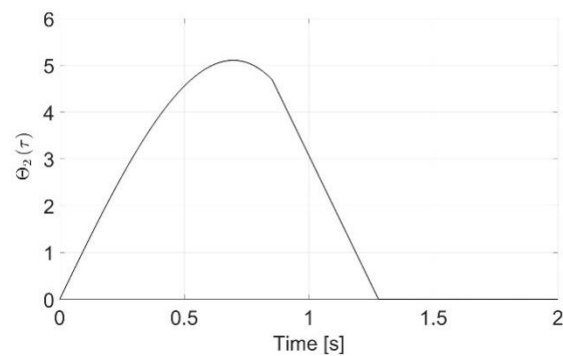

Fig. 2. System's position

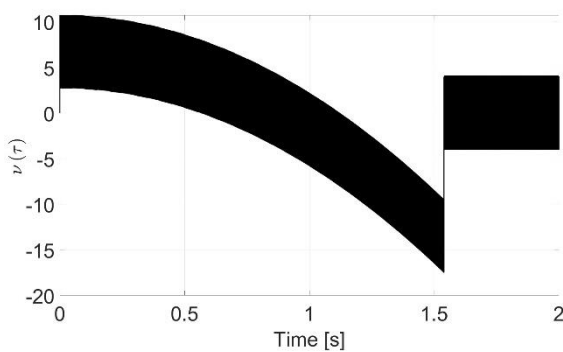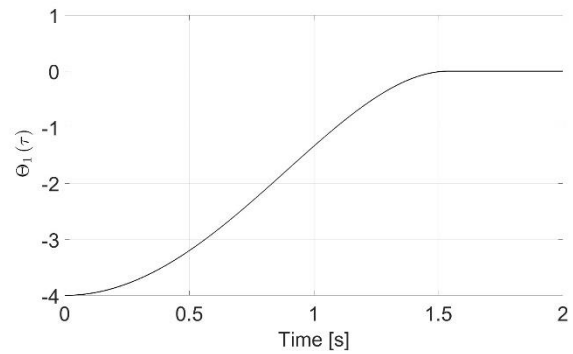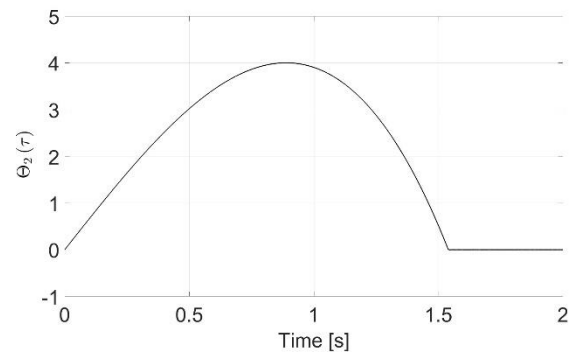**Fig. 3.** System's velocity

Fig. 4. Control signal

System's position (Figure 5) and velocity behave similarly as in the first case. However, one can observe from Fig. 6 that the limitation of the system's velocity is fulfilled. This is the reason why in this case the regulation time is longer than that in the scenario when the control signal is constrained. The last case covers both control signal and velocity limitations. Minimised ITAE is given as follows:

$$E = 1.5805. \tag{64}$$
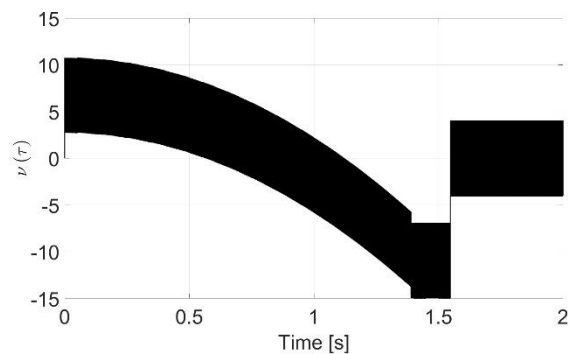

Fig. 5. System's position

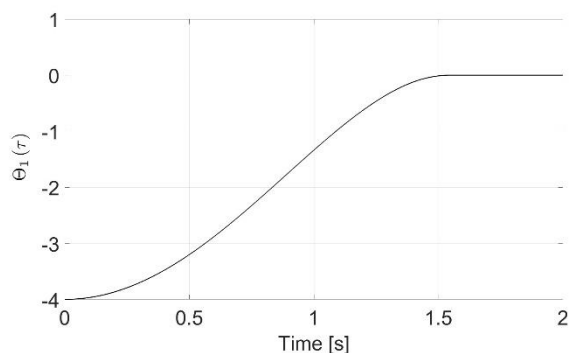**Fig. 6.** System's velocity

Fig. 7. Control signal
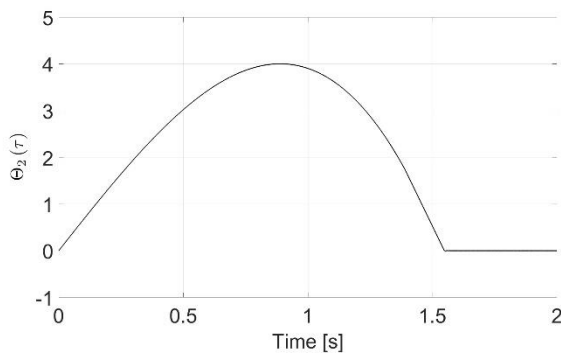

Fig. 8. System's position

Fig. 9. System's velocity

We can see that it is the highest value of all three scenarios, which is a logical outcome due to the fact that now we have to provide the fulfilment of not one but two limitations. Optimal switching curve parameters are as follows:

$$\begin{cases} \gamma = 3.3750 \\ \tau_0 = 0.8528s \end{cases} \tag{65}$$

The regulation time is $\tau_f = 1.5477$. Again, one can observe that in order to satisfy both constraints, we select the minimum value of γ from both scenarios and the regulation time is the longest one from all three cases. From Figs. 7, 8 and 9, we can see that control signal and system state behave as we expected, and both control signal and velocity limitations are provided. The chattering visible in the control signal in Figs. 1, 4 and 7 could be reduced by changing the sign function of the sliding variable in Eq. (6) to a saturation function. In this paper, we have chosen not to do this to present the main contributions of our approach more clearly. Moreover, unfortunately, using the saturation function would result in a quasi-sliding motion instead of an ideal one. Namely, the state would be constrained to a close vicinity of the sliding line, not necessarily directly to it.

6. CONCLUSIONS

This work comprises the design of a sliding mode controller which can be applied for second-order, nonlinear systems. A switching curve that ensures the elimination of the reaching phase and the robustness for the whole control process is introduced. A finite time convergence of the representative point to the demand state is ensured. Control signal and system's velocity are both constrained separately, and after that, this approach is combined. In order to achieve a satisfying dynamical performance of the system, the ITAE quality index is minimised. It is noticeable that the main difficulty of the approach was considering all the possible scenarios and calculating the optimal parameter values for all of them. However, once this is done, the approach can be used fairly easily, using the final results presented above. Comparing the approach applied in this article with the one used in [14], one can conclude that IAE quality index treats the plant error similarly throughout the whole control process, while ITAE penalises the error more for further time periods. This results in obtaining slightly higher initial values of error for ITAE quality index. However, these values decrease more rapidly.

REFERENCES

1. Ali N, Liu Z, Armghan H, Ahmad I, Hou Y. LCC-S-Based integral terminal sliding mode controller for a hybrid energy storage system using a wireless power system. Energies. 2021;14: 1693.
2. Chang TH, Hurmuzlu Y. Trajectory tracking in robotic systems using variable structure control without a reaching phase, 1992 American Control Conference. IEEE. 1992;1505–1509.
3. Chang TH, Hurmuzlu Y. Sliding control without reaching phase and its application to bipedal locomotion. Journal of Dynamic Systems. Measurement and Control. 1993, 115(3):447–455.
4. Chen Y, Bu W, Qiao Y. Research on the Speed Sliding Mode Observation Method of a Bearingless Induction Motor, Energies. 2021:14.
5. Clemente A, Montiel M, Barreras F, Lozano A, Costa-Castello R, Vanadium Redox Flow Battery State of Charge Estimation Using a Concentration Model and a Sliding Mode Observer. IEEE Access. 2021;9:72368–72376.
6. Drazenović B. The invariance conditions in variable structure systems, Automatica.1969;5(3):287–295.
7. El-Sousy FFM, Alenizi FAF. Optimal Adaptive Super-Twisting Sliding-Mode Control Using Online Actor-Critic Neural Networks for Permanent-Magnet Synchronous Motor Drives, IEEE Access, 2021; 9:82508–82534.
8. Hu J, Zhang H, Liu H, Yu X. A survey on sliding mode control for networked control systems. International Journal of Systems Science. 2021;52(6):1129–1147.
9. Incremona GP, Rubagotti M, Tanelli M, Ferrara A. A general framework for switched and variable-gain higher-order sliding mode control, IEEE Trans. on Aut. Contr. 2020;66(4):1717–1724.
10. Komurcugil H. A new sliding mode control for single-phase UPS inverters based on rotating sliding surface. IEEE International Symposium on Industrial Electronics. 2010;579–584.
11. Komurcugil H. Rotating-sliding-line-based sliding-mode control for single-phase UPS Inverters. IEEE Transactions on Industrial Electronics. 2012;59(10):3719–3726.
12. Li H, Chen X, Zhang H, Cui X. High-Precision Speed Control for Low-Speed Gimbal Systems Using Discrete Sliding Mode Observer and Controller. IEEE Trans. Emerg. Sel. Topics Power Electron. 2022; 10:2871–2880.
13. Pietrala M, Leśniewski P, Bartoszewicz A. Sliding Mode Control with Minimization of the Regulation Time in the Presence of Control Signal and Velocity Constraints. Energies. 2021;14(10):2887.
14. Pietrala M, Leśniewski P, Bartoszewicz A. IAE Minimization in Sliding Mode Control With Input and Velocity Constraints. IEEE Access. 2022;10:28631–28641.
15. Shang W, Jing G, Zhang D, Chen T, Liang Q. Adaptive Fixed Time Nonsingular Terminal Sliding-Mode Control for Quadrotor Formation With Obstacle and Inter-Quadrotor Avoidance. IEEE Access. 2021; 9: 60640–60657,.
16. Skruch P, Długosz M. Design of terminal sliding mode controllers for disturbed non-linear systems described by matrix differential equations of the second and first orders. Applied Sciences. 2019; 9(11):2325–2344.
17. Tang Y. Terminal sliding mode control for rigid robots. Automatica. 1998;34:51–56.
18. Tran AT, Minh BLN, Huynh VV, Tran PT, Amaefule EN, Phan VD, Nguyen TM. Load Frequency Regulator in Interconnected Power System Using Second-Order Sliding Mode Control Combined with State Estimator. Energies. 2021; 14.
19. Ullah N, Mehmood Y, Aslam J, Ali A, Iqbal J. UAVs-UGV, Leader Follower Formation Using Adaptive Non-Singular Terminal Super Twisting Sliding Mode Control. IEEE Access. 2021;9:74385–74405.
20. Utkin V, Drakunov SV. On discrete-time sliding mode control, Proc. IFAC Conf. Nonlinear Control. 1989;484–489.
21. Wang Y, Feng Y, Zhang X, Liang J. A new reaching law for antidisturbance sliding-mode control of PMSM speed regulation system. IEEE Trans. Power Electron. 2020;35(4):4117–4126.

22. Wang T, Tan N, Zhang X, Li G, Su S, Zhou J, Qiu J, Wu Z, Zhai Y, Labati RD, Piuri V, Scotti F. A Time-Varying Sliding Mode Control Method for Distributed-Mass Double Pendulum Bridge Crane With Variable Parameters. IEEE Access. 2021;9:75981–75992.

23. Wang P, Xu Y, Ding R, Liu W, Shu S, Yang X. Multi-Kernel Neural Network Sliding Mode Control for Permanent Magnet Linear Synchronous Motors. IEEE Access. 2021;9:57385–57392.

24. Xu L, Shao X, Zhang W. USDE-Based Continuous Sliding Mode Control for Quadrotor Attitude Regulation: Method and Application. IEEE Access. 2021;9:64153–64164.

25. Yousufzai IK, Waheed F, Khan Q, Bhatti AI, Ullah R, Akmeliawati R. A Linear Parameter Varying Strategy Based Integral Sliding Mode Control Protocol Development and Its Implementation on Ball and Beam Balancer. IEEE Access. 2021;9:74437–74445.

26. Zhihong M, Yu XH, Terminal sliding mode control of MIMO linear systems. IEEE Transactions on Circuits and Systems I: Fundamental Theory and Applications. 1997;44:1065–1070.

Mateusz Pietrala: https://orcid.org/0009-0008-6715-4967

Piotr Leśniewski: https://orcid.org/0000-0003-4131-6928

Andrzej Bartoszewicz: https://orcid.org/0000-0002-1271-8488